

different matrix for the right multiplication. The interesting property here is that all the left multiplication matrices commute with all the right multiplication matrices.²⁰ Now consider the action of the group elements on the cosets. The left multiplication permutes the cosets (see eq 6), but the right multiplication

$$gxH = x'H \quad (6)$$

(usually) breaks up the cosets (see eq 7). The left multiplication

$$xHg = \text{parts of several cosets} \quad (7)$$

on cosets can be represented by permutation matrices. The effect of the right multiplication on cosets is also represented by matrices called double-coset matrices. The left multiplication matrices commute with the double-coset matrices.²¹ The double-coset matrices are the incidence matrices of "topological representations" which pictorially display isomer (coset) interconversion.²² For the purposes here these topological representations can be considered as "nets" in the coordinate space in which the points are isomers and the edges symbolize paths between them. The key result is that the left multiplication matrices (permutation of identical atoms) commute with the topological representations and are therefore symmetries of the coordinate space. These double-coset matrices are symmetric across the principle diagonal if the double coset is self-inverse.²¹

A5. Combinatorics. Table II was constructed by using two previously published combinatorial formulas. Ruch²³ has given a formula for the total number of double cosets of a subgroup P in G . Frame¹⁸ has given a formula for the number of self-inverse double cosets. The percentages in Table II for n larger than 5 were obtained by dividing the two numbers. This is only a good approximation for the number of possible SI and NSI processes since the sizes of double cosets vary. A formula which gives sizes

of double cosets and does not need double-coset representatives is lacking. For n less than 5 the percentages are exact and were enumerated by generation of the various possibilities.

A6. Conjugation Invariance, Invariance to Choice of Reference Isomer and Atom Numbering. Changing the reference isomer or renumbering the atoms in a given problem has the effect of conjugation by the permutation, r , which expresses the change of numbering in eq 8. The operation of conjugation preserves

$$r^{-1}xr = x' \quad (8)$$

all the group-theoretical properties being used in the present work. These are the self-inverse property of cosets and double cosets, the size of double cosets, the cycle structure and order of a permutation, and the combinatorial results.

A7. Method for Computing the Largest Transition-State Symmetry Group. Consider a reference structure and another isomer. The symmetries common to both are the elements of the group intersection (eq 9) where P is the symmetry group of the

$$P \wedge x^{-1}Px \quad (9)$$

reference isomer, x is in the coset representing the other isomer, and $x^{-1}Px$ is the symmetry group of the other isomer. If x is an element of order 2 or a member of an inverse pair in the coset representing the nonreference isomer (and therefore exchanges the two isomers by left multiplication), then multiplication by any element, y , in the intersection group (which therefore fixes both isomers by left multiplication) will give another element which exchanges the two isomers. Repetition of this procedure for all members of the intersection group will give a group of size twice that of the intersection group and will include all the permutations which fix both isomers and all those which exchange them (there will be an equal number of each).

Structural Studies of Silicates by Solid-State High-Resolution ²⁹Si NMR

E. Lippmaa,* M. Mägi, A. Samoson,^{1a} G. Engelhardt,^{1b} and A.-R. Grimmer^{1c}

Contribution from the Department of Physics, Institute of Cybernetics of the Estonian Academy of Sciences, Tallinn 200001, USSR, and the Central Institute of Physical Chemistry and the Central Institute of Inorganic Chemistry of the Academy of Sciences of the GDR, Berlin-Adlershof, East Germany. Received December 27, 1979

Abstract: The high-resolution ²⁹Si NMR spectra of solid silicates and aluminosilicates have been studied. High-speed magic angle sample spinning in combination with high-power proton decoupling and, wherever possible, polarization transfer was used to achieve high (1 ppm) resolution. Although ionization and cation influence are reflected on ²⁹Si chemical shifts, the isotropic ²⁹Si chemical shifts in solids and solutions are generally the same and depend mainly on the degree of condensation of silicon-oxygen tetrahedra. In solid aluminosilicates, additional paramagnetic shifts appear, which correlate well with the degree of silicon substitution by aluminum.

Introduction

We recently reported the results of preliminary experiments with solid-state high-resolution NMR spectroscopy of some representative groups of organic and inorganic compounds.² In this paper, we describe the results of further studies of solid silicates, which show that the very considerable possibilities of high-resolution NMR are not confined to liquids, solutions, and solid samples of predominantly organic compounds, but these techniques are perfectly well applicable to the study and analysis of solid,

insoluble inorganic silicates and aluminosilicates.

High-resolution ²⁹Si NMR has proved to be an efficient method for structure elucidation of silicic acids and silicate anions in solution. Numerous studies of alkali-^{3,4} and tetraalkylammonium silicates⁵ as well as solutions of silicic acids^{6,7} have established

(3) G. Engelhardt, D. Zeigan, H. Jancke, D. Hoebbel, and W. Wicker, *Z. Anorg. Allg. Chem.*, **418**, 17 (1975).

(4) R. K. Harris and R. H. Newman, *J. Chem. Soc., Faraday Trans. 2*, **73**, 1204 (1977).

(5) D. D. Hoebbel, G. Garzö, G. Engelhardt, R. Ebert, E. Lippmaa, and M. Alla, *Z. Anorg. Allg. Chem.*, in press.

(6) D. Hoebbel, G. Garzö, G. Engelhardt, and A. Till, *Z. Anorg. Allg. Chem.*, **450**, 5 (1979).

(7) G. Engelhardt, W. Altenburg, D. Hoebbel, and W. Wicker, *Z. Anorg. Allg. Chem.*, **437**, 249 (1977).

(1) (a) Institute of Cybernetics; (b) Institute of Physical Chemistry; (c) Institute of Inorganic Chemistry.

(2) E. T. Lippmaa, M. A. Alla, T. J. Pehk, and G. Engelhardt, *J. Am. Chem. Soc.*, **100**, 1929 (1978).

Table I. ^{29}Si Isotropic Shifts in Solid Silicates (ppm from Me_4Si)

compd	type of silicon-oxygen tetrahedra	Q ⁰ single tetrahedra	Q ¹ end group	Q ² middle group	Q ³ branching site	Q ⁴ cross-linking group
NaH_3SiO_4	single	-66.4				
$\text{Na}_2\text{H}_2\text{SiO}_4 \cdot 8.5\text{H}_2\text{O}$	single	-67.8				
CaNaHSiO_4	single	-73.5				
$(\text{CaOH})\text{CaHSiO}_4$	single	-72.5				
$\text{Zn}_2(\text{OH})_2[\text{Si}_2\text{O}_7] \cdot \text{H}_2\text{O}$ (hemimorphite)	double		-77.9			
$\text{Ca}_6(\text{OH})_6[\text{Si}_2\text{O}_7]$	double		-82.6			
$\text{K}_4\text{H}_4[\text{Si}_4\text{O}_{12}]$	cyclotetra			-87.5		
$\text{Ca}_2(\text{OH})_2[\text{SiO}_3]$ (hillebrandite)	single chain			-86.3		
$\text{Ca}_4(\text{OH})_2[\text{Si}_3\text{O}_9]$ (foshagite)	single chain			-86.5		
$\text{Ca}_3[\text{Si}_3\text{O}_9]$ (wollastonite)	single chain			-88.0		
$\text{Ca}_2\text{NaH}[\text{Si}_3\text{O}_9]$ (pectolite)	single chain			-86.3		
$\text{Ca}_6(\text{OH})_2[\text{Si}_6\text{O}_{17}]$ (xonotlite)	double chain			-86.8	-97.8	
$\text{Mg}_3(\text{OH})_2[\text{Si}_3\text{O}_{10}]$ (talc)	layer				-98.1	
$(\text{Me}_4\text{N})_8[\text{Si}_8\text{O}_{20}]$	double four-ring				-99.3	
$(\text{Et}_4\text{N})_6[\text{Si}_6\text{O}_{15}]$	double three-ring				-90.4	
SiO_2 (low quartz)	spiral					-107.4
SiO_2 (low cristobalite)	three-dimensional six-rings					-109.9

the identities of a whole series of silicate anions of different structure, due to polycondensation of the silicates. The total range of ^{29}Si chemical shifts in silicates is appreciable, from -60 to -120 ppm, with analytically significant subdivision into well-separated ranges for monosilicates (Q⁰), disilicates and chain end groups (Q¹), middle groups in chains (Q²), chain branching sites (Q³), and the three-dimensional cross-linked framework (Q⁴).⁸

In solid silicates, dipolar interactions between nuclear spins and anisotropy of the ^{29}Si chemical shifts lead to excessive NMR line widths and to weak, completely overlapping lines, if conventional CW or FT NMR methods are used. The 208-ppm ^{29}Si NMR line width⁹ measured in solid $\text{Na}_2\text{Si}_2\text{O}_5$ by far exceeds the total range of ^{29}Si chemical shifts in silicates. Line widths of this size have made ^{29}Si NMR impractical as a general method for structural studies of solid silicates, although the early measurements of Holzman, Lauterbur, et al.¹⁰ on cristobalite (-113 ± 2 ppm) and quartz (-109 ± 2 ppm) must be mentioned. Because of absence of protons and a nearly symmetric ^{29}Si shielding tensor, line broadening is not as severe in quartz as it is in silicates. Other techniques, such as the kinetics of formation of polyoxo anions with molybdate ion,¹¹ paper chromatography,¹¹ and the formation of trimethylsilyl derivatives,¹² have been used for structural studies of silicate anions. Quite obviously, all these methods are suitable only for the study of solutions. Unfortunately, all methods involving dissolving a solid silicate are unreliable owing to unavoidable hydrolysis and further condensation of the silicate anions. The same holds for the ^{29}Si FT NMR of solutions. X-ray analysis is certainly the best option, but can be used only with crystalline samples and is rather unreliable in differentiating between the silicon and aluminum sites in the crystal unit cell.

As was shown in our first paper,² a combination of rapid sample spinning at magic angle to the direction of the external polarizing magnetic field with high-power ^1H spin decoupling and polarization transfer in the rotating frame provides a practical method for obtaining high-resolution NMR spectra of spin 1/2 nuclei in amorphous and microcrystalline solids and powders.¹³ If the

strong magnetic field of a superconducting solenoid is used in these experiments, reasonably good sensitivity can be achieved in addition to high resolution and large chemical shifts. The main problems in these solid-state high-resolution NMR studies are possible specific solid state effects—i.e., differences between the isotropic ^{29}Si chemical shifts of equivalent structural units in solids and the corresponding solutions, and the problem of interpretation of such chemical shifts where no parallels with solutions are possible owing to complete insolubility of the compounds, such as aluminosilicates.

Experimental Section

Materials and Samples for NMR Measurements. The silicates were pure synthetic compounds, prepared according to classical synthetic procedures. All aluminosilicates were natural minerals, donated by the collection of the Tallinn Technical University. All compounds were studied as fine powders, prepared manually in agate mortar.

Instrumentation. All ^{29}Si NMR spectra were recorded in a 47-kG field at 39.74 MHz on a Bruker-Physik CXP-200/300 solid-state high-resolution NMR spectrometer, equipped with an Aspect-2000 data system. The standard ^{13}C proton-enhanced magic angle sample spinning probe was slightly modified for this purpose. The conical Andrew-type rotors, manufactured from Delrin, were found to be suitable for ^{29}Si measurements, because, owing to the generally small anisotropy of the ^{29}Si chemical shifts, no extremely high rotation angle stability is needed and the rotor material is completely silicon-free. The rotor spinning rate was close to 3000 Hz. Whether cross-polarization can be used to enhance sensitivity depends upon the availability of protons in constituent water, the hydroxyl groups, or even in the adsorbed water. Wherever possible, proton-enhanced resonance with decoupling was used, but some water-free samples were studied with the use of the conventional FT NMR technique with high-power ^1H spin decoupling and rapid sample spinning at the magic angle. Even with high-power proton decoupling, but without rapid sample spinning, the residual line widths tend to remain large. In NaH_3SiO_4 , a typical monosilicate, the line width at half height equaled 2.2 ppm with rapid sample spinning and 41.0 ppm with a stationary sample. The ^{29}Si line widths were usually of the order of 1–2 ppm. In some cases (cyclic tetraalkylammonium silicates) even 10-Hz (0.25 ppm) line widths were achieved. All measurements were carried out at 35 °C temperature with the trimethylsilyl ester of double four-ring octameric silicate Q_8M_8 or liquid M_2 ($\text{Me}_3\text{SiOSiMe}_3$) used as secondary standards for the ^{29}Si chemical shifts, which were related to external Me_4Si with the low-field paramagnetic shifts positive. The ^{29}Si chemical shift $\delta(^{29}\text{Si})$ of the trimethylsilyl groups M was taken to equal +11.5 ppm from external liquid Me_4Si in solid Q_8M_8 and +6.6 ppm in liquid M_2 , with no corrections for different volume susceptibilities. The ^1H and ^{29}Si spin-lattice relaxation times were found to be surprisingly short, especially in the protonated species. Short 1–2-s time intervals between the rf pulse sequences were used in this case and only up to 30-s intervals between the rf pulses in the experiments without cross-polarization, but with magic-angle spinning. From 200 to 8000 FIDs were accumulated. The total measuring time was a few minutes in most cases and rarely exceeded 2 h. The ^1H - ^{29}Si spin contact time with the Hartmann-Hahn condition fulfilled in the rotating frame was typically about 5 ms, but was optim-

(8) All silicates anions can be described as a combination of Q units, since this symbol is used to represent a silicon atom bonded to four oxygen atoms, $\text{Q} = \text{Si}(\text{O}_{1/2})_4$. The superscript shows the number of other Q units (silicon-oxygen tetrahedra) attached to the silicon tetrahedron under study.

(9) B. D. Mosel, W. Müller-Warmuth, and H. Dutz, *Phys. Chem. Glasses*, **15**, 154 (1974).

(10) G. R. Holzman, P. C. Lauterbur, J. H. Anderson, and W. Koth, *J. Chem. Phys.*, **25**, 172 (1956).

(11) W. Wieker and D. Hoebbel, *Z. Anorg. Allg. Chem.*, **366**, 139 (1969).

(12) C. W. Lentz, *Inorg. Chem.*, **3**, 574 (1964).

(13) E. Lippmaa, *Usp. Fiz. Nauk*, **120**, 512 (1976); J. Schaefer and E. O. Stejskal, *J. Am. Chem. Soc.*, **98**, 1031 (1976); E. Lippmaa, M. Alla, and T. Tuherm in "Magnetic Resonance and Related Phenomena", Proceedings of the 19th Congress AMPERE, H. Brunner, K. H. Hausser, and D. Schweitzer, Eds., Heidelberg-Geneva, 1976.

Table II. ^{29}Si Isotropic Shifts in Solid Aluminosilicates (ppm from Me_4Si)

compd	Al:Si ratio in the lattice	Q ³ . . . Al ^a		Q ⁴				
		1 Al ^b	0 Al	4 Al	3 Al	2 Al	1 Al	0 Al
$\text{Al}_2(\text{OH})_2[\text{Si}_4\text{O}_{10}]$ (pyrophyllite)	0		-91.5 -95.0					
$\text{KAl}_2(\text{OH})_2[\text{AlSi}_3\text{O}_{10}]$ (muscovite)	1:3	-84.6 ^c -86.7 ^c						
SiO_2 (low quartz)	0							-107.4
$\text{Na}[\text{AlSi}_3\text{O}_8]$ (albite)	1:3					-92.5	-96.7 -104.2	
$\text{K}[\text{AlSi}_3\text{O}_8]$ (orthoclase)	1:3					-95 ^c	-98 ^c -101 ^c	
$\text{K}[\text{AlSi}_3\text{O}_8]$ (adular)	1:3					-95 ^c	-98.2 ^c -100.5 ^c	
$\text{K}[\text{AlSi}_3\text{O}_8]$ (sanidine)	1:3					-95.7 ^c	-96.8 ^c -100.9 ^c	
$\text{Na}_2[\text{Al}_2\text{Si}_3\text{O}_{10}]\cdot 2\text{H}_2\text{O}$ (natrolite)	2:3				-87.7	-95.4		
$\text{KNa}_3[\text{AlSiO}_4]_4$ (nepheline)	1:1			-84.8	-88.4 ^d			
$\text{Ca}[\text{Al}_2\text{Si}_2\text{O}_8]$ (anorthite)	1:1			-83.1 ^c				

^a Six-coordinated aluminum. ^b Four-coordinated aluminum. ^c Broadened lines. ^d Signal of low intensity.

ized in the range between 0.5 and 12 ms. Even quite similar structures can have widely different optimal spin contact times. The ^{29}Si $\pi/2$ rf pulse amplitude equaled 7–10 μs .

Results

The solid-state isotropic ^{29}Si chemical shifts in some typical silicates are given in Table I and the isotropic shifts in solid aluminosilicates in Table II. A few representative ^{29}Si NMR spectra are given in Figures 2–4. The first group of compounds contains all the common types of silicate anions, thus providing possibilities for direct comparison with the ^{29}Si chemical shifts of the same anions, measured in solution. All compounds shown in Table I contain only big cations (Na, K, Ca, Mg, Zn, and the alkylammonium ions), which cannot substitute for silicon in the silicate framework.

Table II contains data for layered structures, consisting of Q³ units in a honeycomb network of hexameric rings and of aluminosilicates with a three-dimensional framework, consisting of Q⁴ units with partial substitution of some silicon atoms by aluminum.¹⁴ The number of such substitutions is shown in Table II underneath the Q³ and Q⁴ symbols. In the last case the cations again have big ionic radii.

In most cases the measured spectra consisted of a few sharp lines, similar to those depicted in Figures 3 and 4. The ^{29}Si isotropic chemical shifts could be resolved and measured to ± 0.1 ppm. In the case of nonequivalent silicon–oxygen tetrahedra, such as Q² and Q³, or tetrahedra of the same type, but of a different degree of aluminum substitution in the second coordination sphere, such as Q⁴(3Al) and Q⁴(2Al), two or more ^{29}Si lines were registered in the NMR spectrum. The line intensities were in qualitative agreement with the relative abundance of each particular unit in the aluminosilicate anion. For quantitative accuracy, allowances must be made for different relaxation times, which reduces sensitivity.

Discussion

It is immediately obvious from the data presented in Table I that the solid-state isotropic ^{29}Si chemical shift values are determined primarily by the type of condensation of the silicon–oxygen tetrahedra. Increasing condensation from the single to double tetrahedra, to chains and cyclic layered structures, and finally to three-dimensional frameworks leads to increasing diamagnetic shielding of the ^{29}Si nucleus and very closely parallels the same phenomenon in solutions of the same anions, as illustrated in Figure 1. Again, there are well-separated and analytically useful ranges for each type of Q units. The somewhat smaller shift ranges shown for solids may be caused by the smaller number

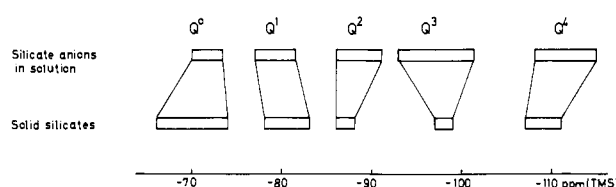


Figure 1. Ranges of ^{29}Si chemical shifts of different structural units of silicate anions in solid silicates and silicate solutions.

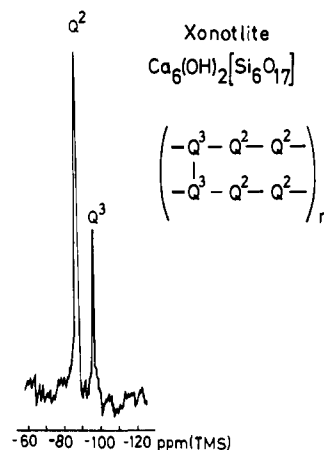


Figure 2. Solid state ^{29}Si NMR spectrum of xonotlite.

of solid samples studied. The data for silicate anions in solution are taken from ref 3, 4, 7, and 15. These relationships, which establish a direct link to the large body of data for silicate solutions, hold true for solids containing only big cations (alkali metals, alkaline earths, and tetraalkylammonium cations), which have only a minor influence upon the ^{29}Si chemical shifts of the silicate anions. An increasing number of acidic protons lead to a small paramagnetic shift, as does substitution of calcium by sodium. The small cation influence in solids is in agreement with the rather modest pH³ and cation¹⁶ dependence of the chemical shifts of silicate anions in solution.

Just as in organic siloxanes,¹⁷ trimethylsilyl esters of silicic acid,¹⁸ and solutions of silicates,^{3,5} the formation of a three-

(15) G. Engelhardt, W. Altenburg, D. Hoebbel, and W. Wieker, *Z. Anorg. Allg. Chem.*, **428**, 43 (1977).

(16) G. Engelhardt and D. Hoebbel, unpublished results.

(17) G. Engelhardt, H. Jancke, M. Mägi, T. Pehk, and E. Lippmaa, *J. Organomet. Chem.*, **28**, 293 (1971).

(18) D. Hoebbel, G. Garzó, G. Engelhardt, H. Jancke, P. Franke, and W. Wieker, *Z. Anorg. Allg. Chem.*, **424**, 115 (1976).

(14) H. Strunz, "Mineralogische Tabellen", Akad. Verlag Geest & Portig K.-G., Leipzig, 1957.

membered ring of silicon-oxygen tetrahedra leads to a ~ 9 -ppm paramagnetic shift. Such shifts are small in larger rings, but even in quartz and cristobalite the ^{29}Si shieldings differ by about 3 ppm.

The spectrum shown in Figure 2 illustrates the possibilities of ^{29}Si solid state NMR in structural studies of silicates. The two-line spectrum of xonotlite with a 2:1 line intensity ratio reflects well the structure of this double-chain silicate, branched at every third silicon with a 2:1 ratio of the contents of Q^2 and Q^3 groups. The spectra of different types of Portland cements show up to four signals in the range between -69 and -74 ppm, typical in single silicate tetrahedra. The different signals in one and the same sample can be explained by structural effects produced by irregular distribution of cations, hydration, or different structural relations between the SiO_4 tetrahedra. Naturally, the solid-state ^{29}Si NMR should offer new and interesting possibilities for the investigation of many problems of cement chemistry in general. Studies of such type are in preparation and first results will be reported soon.

It must be mentioned that differences have been found earlier between the ^{29}Si chemical shifts in solid calcium silicates and the equivalent silicate anions in solutions by broad-line NMR. This method, however, is not easily applicable to the exact measurement of ^{29}Si chemical shifts, because the anisotropic line shape together with a poor signal to noise ratio leads to significant uncertainties in the calculation of the isotropic shift value. The differences stated in ref 19 are caused by such errors.

The data in Table II illustrate the influence of a typical small cation, aluminum, which can easily participate in the silicate structure both as a six-coordinated cation and in the four-coordinated form, replacing silicon in the lattice. Comparison of the ^{29}Si chemical shifts in talc (Table I), pyrophyllite, and muscovite (Table II) provides a good example for the twofold aluminum influence on the ^{29}Si chemical shifts. Talc contains double silicate layers,¹⁴ consisting of Q^3 units in a honeycomb network of hexameric rings with magnesium occupying all the cationic sites between the two layers. These hamburger-like sandwiches are held together by van der Waals forces only, which contributes to the soft feel and pliability of talc. All Q^3 units are equivalent and the ^{29}Si NMR spectrum contains only one single line at -98.1 ppm, well inside the normal shift range for the Q^3 units (see Table I).

Replacement of magnesium by six-coordinated aluminum between the silicate layers as in pyrophyllite leads to an unequal two out of three occupancy by aluminum of the cationic sites of the layers,¹⁴ which leads to ^{29}Si line splitting together with a significant paramagnetic shift. A tentative assignment of the lines can be done by the assumption that the silicon-oxygen tetrahedra close to the aluminum octahedra exert a stronger paramagnetic shift ($\delta -91.5$ ppm) than the less perturbed Q^3 units, where a shift close to that found in talc could be expected. Replacement of one-fourth of the silicon atoms by four-coordinated aluminum in the silicate layers, as in mica¹⁴ (muscovite), retains the basic structure and the ^{29}Si line splitting, but an additional paramagnetic shift and considerable line broadening appear. The paramagnetic shift is caused by replacement of silicon by aluminum in the second coordination sphere [$\text{Q}^3(1\text{Al})$ instead of $\text{Q}^3(0\text{Al})$] around the silicon, and line broadening can be taken to reflect the irregular structure of the layers and thus also of the further coordination spheres around each $\text{Q}^3(1\text{Al})$ silicon atom, caused by the introduction of aluminum into the silicate layer. This effect is a very general phenomenon and is also present in the ^{29}Si spectra of tectosilicates, such as sanidine (Figure 4), with an irregular Si/Al distribution. The interlayer six-coordinated aluminum is present in both pyrophyllite and muscovite, and should be expected to exert a similar influence upon the Q^3 ^{29}Si chemical shifts.

The strong paramagnetic influence of four-coordinated aluminum in case of substitution for silicon in the second coordination sphere of silicon is further corroborated by ^{29}Si spectra of a group of three-dimensional aluminosilicates—albite, orthoclase, natrolite, and nepheline, with different Al:Si ratios. These aluminosilicates contain several inequivalent Q^4 units of different degree of alu-

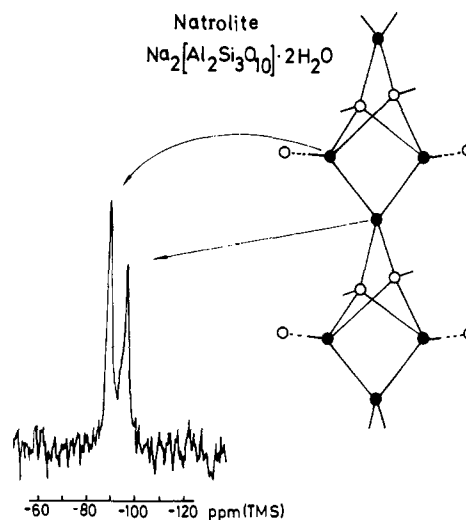


Figure 3. Solid state ^{29}Si NMR spectrum and schematic structure of natrolite (\bullet , silicon; \circ , aluminum; only the central atoms of the tetrahedra are shown).

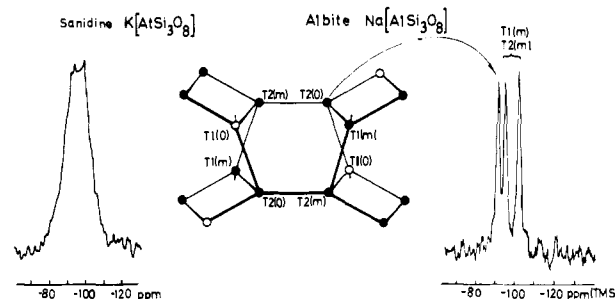


Figure 4. Solid state ^{29}Si NMR spectra of sanidine and albite. The crystal unit cell of alkali feldspars²² is represented as having an ideally ordered Al/Si distribution with 100% Al in the site T1 (\circ , silicon; \bullet , aluminum; only the central atoms of the tetrahedra are shown).

minum substitution with widely different ^{29}Si chemical shifts, as shown in Table II and illustrated in Figures 3 and 4. It follows from Tables I and II that five different, but nearly overlapping, chemical-shift ranges can again be found for the different Q^4 units with the total shift difference of 25 ppm. $\text{Q}^4(0\text{Al})$ is represented by quartz and cristobalite, and the fully aluminum-substituted $\text{Q}^4(4\text{Al})$ by the strongest ^{29}Si line in the spectrum of nepheline.

The ^{29}Si NMR spectra are in good agreement with the known X-ray structures of these aluminosilicates. The structure of natrolite²⁰ (Figure 3) contains silicon atoms of two types—those connected to three aluminum-oxygen tetrahedra $\text{Q}^4(3\text{Al})$ and those with two substitutions $\text{Q}^4(2\text{Al})$, in a 2:1 ratio. The same line intensity ratio is present in the ^{29}Si NMR spectrum, thus allowing unequivocal assignment of these lines. The more complicated structure of albite,^{21,22} with three inequivalent silicon sites, is depicted in Figure 4. The structure of albite is known to be regular, with more than 90% of the aluminum in position T1 (\circ) of the four-ring.^{21,23} This allows one to assign the most paramagnetic ^{29}Si resonance at -92.5 ppm to a $\text{Q}^4(2\text{Al})$ tetrahedron in position T2 (\circ), and the remaining two lines to two $\text{Q}^4(1\text{Al})$ units T2 (m) and T1 (m) with different geometry and cation influence. As befits the regular structure of albite, the ^{29}Si lines are sharp and well separated. Orthoclase is known to have a less orderly Al:Si distribution on the lattice,²² and the ^{29}Si lines are broader and less well separated. The regularity of Si/Al dis-

(20) W. M. Meier, *Z. Kristallogr., Kristallgeom., Kristallphys., Kristalchem.*, **113**, 430 (1960).

(21) P. P. Williams and H. D. Megaw, *Acta Crystallogr.*, **17**, 882 (1964).

(22) F. Laves, *Z. Kristallogr., Kristallgeom., Kristallphys., Kristalchem.*, **113**, 265 (1960).

(23) E. Brun, P. Hartmann, H. H. Staub, St. Hafner, and F. Laves, *Z. Kristallogr., Kristallgeom., Kristallphys., Kristalchem.*, **113**, 65 (1960).

(19) E. Fechner, A.-R. Grimmer, and W. Wieker, *Z. Chem.*, **18**, 419 (1978).

tribution in the lattice diminishes from nearly complete order in albite through orthoclase and adular to the disordered sanidine.²² In the last three cases the ²⁹Si lines are no longer separated, but the presence of several separate resonances is still apparent; see Figure 4.

In accordance with the Loewenstein rule,²⁴ only Q⁴ (4Al) units should be present in pure nepheline with a 1:1 Al:Si ratio. The strongest line at -84.8 ppm fits this assumption well, and the small shoulder at -88.4 ppm is likely to be caused by Q⁴ (3Al) groups, present in the natural mineral owing to deviations from the ideal 1:1 Al:Si ratio.²⁵ The Q⁴ (4Al) groups are the main structure elements of the anorthite lattice as well. The ²⁹Si chemical shift

(-83.1 ppm) is close to that found in nepheline. No additional lines were found, but the resonance was asymmetrically broadened with some weak, unresolved contribution from diamagnetically shifted Q⁴ (3Al) units.

In all cases, a regular paramagnetic shift accompanies increasing substitution of silicon by aluminum in the Q⁴ units. These shifts, and the corresponding shift increments, are peculiar to the solid state and have no counterparts in the ²⁹Si NMR spectra of solutions. Preliminary studies of zeolites have shown that the above-mentioned relationships are quite general and that ²⁹Si chemical shifts can well be used in structural studies of aluminosilicates and related inorganic compounds.

Acknowledgments. We would like to thank Drs. D. Hoebbel, H. Stade, and D. Rademacher for the synthetic silicates and Dr. A. Reier for the aluminosilicates used in this study.

(24) W. Loewenstein, *Am. Mineral.*, **39**, 92 (1954).

(25) T. Hahn and M. J. Buerger, *Z. Kristallogr., Kristallgeom., Kristallphys., Kristallchem.*, **106**, 308 (1955).

Electron Paramagnetic Resonance Detection of Carotenoid Triplet States

Harry A. Frank,* John D. Bolt, Silvia M. de B. Costa,† and Kenneth Sauer

Contribution from the Laboratory of Chemical Biodynamics, Lawrence Berkeley Laboratory, and Department of Chemistry, University of California, Berkeley, California 94720.

Received December 24, 1979

Abstract: Triplet states of carotenoids have been detected by X-band electron paramagnetic resonance (EPR) and are reported here for the first time. The systems in which carotenoid triplets are observed include cells of photosynthetic bacteria, isolated bacteriochlorophyll-protein complexes, and detergent micelles which contain β -carotene. It is well known that if electron transfer is blocked following the initial acceptor in the bacterial photochemical reaction center, back reaction of the primary radical pair produces a bacteriochlorophyll dimer triplet. Previous optical studies have shown that in reaction centers containing carotenoids the bacteriochlorophyll dimer triplet sensitizes the carotenoid triplet. We have observed this carotenoid triplet state by EPR in reaction centers of *Rhodospseudomonas sphaeroides*, strain 2.4.1 (wild type), which contain the carotenoid spheroidene. The zero-field splitting parameters of the triplet spectrum are $|D| = 0.0290 \pm 0.0005 \text{ cm}^{-1}$ and $|E| = 0.0044 \pm 0.0006 \text{ cm}^{-1}$, in contrast with the parameters of the bacteriochlorophyll dimer triplet, which are $|D| = 0.0189 \pm 0.0004 \text{ cm}^{-1}$ and $|E| = 0.0032 \pm 0.0004 \text{ cm}^{-1}$. Bacteriochlorophyll in a light harvesting protein complex from *Rps. sphaeroides*, wild type, also sensitizes carotenoid triplet formation. In whole cells the EPR spectra vary with temperature between 100 and 10 K. Carotenoid triplets also have been observed by EPR in whole cells of *Rps. sphaeroides* and cells of *Rhodospirillum rubrum* which contain the carotenoid spirilloxanthin. Attempts to observe the triplet state EPR spectrum of β -carotene in numerous organic solvents failed. However, in nonionic detergent micelles and in phospholipid bilayer vesicles β -carotene gives a triplet state spectrum with $|D| = 0.0333 \pm 0.0010 \text{ cm}^{-1}$ and $|E| = 0.0037 \pm 0.0010 \text{ cm}^{-1}$.

Introduction

The ubiquity of carotenoids in biological systems is matched in degree by the magnitude of their functional importance. The primary photochemistry in vision is initiated by the absorption of light by the carotenoid retinal¹ The photosynthetic apparatus supplements its light-capturing ability with carotenoid molecules functioning as antenna or light-harvesting pigments which transfer their energy to the reaction center where the primary events of the photosynthetic process occur.² The role of carotenoids as protective devices against irreversible photodestruction from singlet oxygen is well known in photosynthetic bacteria, green plants, and algae.³ However, surprisingly little is known about the excited-state structure of this class of molecules. Recent two-photon and high-resolution vibrational spectroscopic experiments have revealed low-lying excited singlet states of linear polyenes from which fluorescence occurs but into which absorption is forbidden.^{4,5} These observations have challenged theoreticians to explain the

exact origin of these states, and numerous interpretations have been offered.^{6,7}

The triplet state manifold in carotenoid molecules is even less understood. This is due in part to the fact that direct population of the triplet states of isolated carotenoids via singlet-triplet intersystem crossing is not very efficient.^{8,9} Only optical flash photolysis techniques applied to photosensitized carotenoid systems have succeeded in populating the triplet states of these mole-

(1) G. Wald, *Science*, **162**, 230 (1968).

(2) K. Sauer in "Bioenergetics of Photosynthesis", Govindjee, Ed., Academic Press, New York, 1975, pp 115-181.

(3) G. Renger and Ch. Wolff, *Biochim. Biophys. Acta*, **460**, 47 (1977).

(4) R. R. Birge, J. A. Bennett, H. L.-B. Fong, and G. E. Leroi, *Adv. Laser Chem.*, 347-354 (1978).

(5) (a) B. S. Hudson and B. E. Kohler, *Chem. Phys. Lett.*, **14**, 299 (1972);

(b) *J. Chem. Phys.*, **59**, 4984 (1973); (c) R. L. Christensen and B. E. Kohler, *ibid.*, **63**, 1837 (1975).

(6) K. Schulten and M. Karplus, *Chem. Phys. Lett.*, **14**, 305 (1972).

(7) R. R. Birge and B. M. Pierce, *J. Chem. Phys.*, **70**, 165 (1979).

(8) M. Chessin, R. Livingston, and T. G. Truscott, *Trans. Faraday Soc.*, **62**, 1519 (1966).

(9) R. Bensasson, E. J. Land, and B. Maudinas, *Photochem. Photobiol.*, **23**, 189 (1976).

* Department of Chemistry, University of Connecticut, Storrs, Connecticut 06268.

† On leave from Centro de Quimica Estrutural, Complexo I, Instituto Superior Tecnico, Lisboa 1, Portugal.